MULTIAXIAL FATIGUE DAMAGE PREDICTION IN A PROPORTIONAL LOADING CYCLE

ANGHEL CERNESCU , ION DUMITRU, LORAND KUN

Abstract. Mechanical components of in-service machines are frequently subjected to multiaxial cyclic loading, which can result in failure due to the fatigue damage. In general, the multiaxial fatigue life can be predicted based on the stress/strain states variation and using a damage criterion. In this paper, fatigue damage given by a proportional tension-torsion loading cycle is predicted based on proposed methodology. Fatigue damage prediction is made using Findley's criterion on the Mohr's circles of the stress states. The results showed a good capability of the Findley criterion to predict both the critical plane and durability on the analyzed material.

Key words: Multiaxial fatigue, Proportional tension-torsion, Mohr's circle, Findley's criterion, Multiaxial fatigue damage.

1. INTRODUCTION

Fatigue phenomenon is the progressive and localized structural damage which occurs when a material is subject to cyclic loading. The process starts with dislocation movements which form persistent slip bands leading to initiation of cracks that propagates until final failure. Also, this process is carried out over time and defines the durability of a material, respectively component. Depending on the durability domain in which the material is loaded, the life time prediction is quantified by the number of cycles to initiate a crack at a critical point (low-cycle fatigue), or the number of cycles recorded until the final failure, given by the initiation and propagation of a crack from a critical point (high-cycle fatigue or very high cycle fatigue). Basically, the fatigue life prediction of a material represents the damage degree at the end of a loading cycle, which is then cumulated by repeating the loading cycle until the actual failure. Therefore, a major problem in fatigue life prediction is the estimation of the damage caused by a loading cycle. In general, the loading cycle is defined as all the values recorded by the load (forces, moments, pressures, temperatures, etc.), starting from a mean

Mechanics and Strength of Materials, Politehnica University Timisoara

Ro. J. Techn. Sci. – Appl. Mechanics, Vol. 64, N° 1, P. 71–86, Bucharest, 2020

value, recording a maximum, then a minimum and returning to the mean value. The applied cyclic loading determines a stress respectively strain state in material point defined as a multiaxial state. Thus, the stress/strain components vary over time, with the cyclic load variation. At the same time, the multiaxial stress/strain state becomes much more complicated when its components vary in an independent manner or at different frequencies [1–3]. The mode of time variation of the stress/strain state components introduces effects that complicate the prediction of fatigue damage.

Multiaxial loadings are called proportional if the principal directions and the corresponding principal stresses/strains do not change their orientation during a loading cycle. Instead, the multiaxial loadings are called non-proportional if the principal directions and the corresponding principal stresses/strains change their orientation over a loading cycle. Such loadings are very common in the operation of mechanical components, can be complex as a variation over time and it is difficult to quantify their effect on the fatigue life.

Different approaches based on the stress or strain state in the critical point have been developed for fatigue damage prediction at multiaxial loadings. These are based on the following theories: a) maximum principal stress or strain theory [4, 5]; b) maximum shear stress or strain theory [6–8]; c) octahedral shear stress or strain theory [9, 10]. The applicability of one or the other of these theories is especially challenging due to the mechanical behaviour and the different failure modes of materials (tensile or shear failure mode) [11–12] and which is often not easy to know.

In this paper an estimation analysis of fatigue damage produced within a multiaxial loading cycle is performed. The paper contains a stress state analysis in a point on the surface of a multiaxially loaded specimen at tension-torsion, presented in section 2. Then, a fatigue damage prediction given by a proportional tension-torsion loading cycle is presented in section 3. The fatigue damage prediction follows a proposed methodology involving Mohr's circle and a damage criterion.

2. STRESS STATE AT MULTIAXIAL LOADING OF TENSION-TORSION

One of the most common multiaxial fatigue loading is the cyclic tension with torsion. In Fig. 1 is indicated a tubular specimen with thin walls loaded in tension by the forces P and torsion through the torque M_t. The two loads have sinusoidal variation laws. The following stresses act on the orthogonal faces of an infinitesimal element:

$$\sigma_{xx}(t) = \sigma_{xx,a} \cdot \sin(\omega t), \tag{1}$$

$$\sigma_{xy}(t) = \sigma_{xy,a} \cdot \sin\left(\omega t + \delta_{xy}\right), \tag{2}$$

where $\sigma_{xx,a}$ is the amplitude of normal stress, $\sigma_{xy,a}$ is the amplitude of shear stress, $\omega = 2\pi / \mathrm{T} = 2\pi\nu$ is the angular velocity depending on the loading frequency.

The stresses that act on a plane whose normal is inclined with angle Φ with respect to x - axis are:

$$\frac{\sigma_n(t)}{\sigma_{xx,a}} = \frac{1}{2}\left[1 + \cos(2\Phi)\right]\sin(\omega t) + \beta \sin(2\Phi)\sin\left(\omega t + \delta_{xy}\right), \tag{3}$$

$$\frac{\tau_n(t)}{\sigma_{xx,a}} = -\frac{1}{2}\sin(2\Phi)\sin(\omega t) + \beta \cos(2\Phi)\sin\left(\omega t + \delta_{xy}\right), \tag{4}$$

where $\beta = \sigma_{xy,a} / \sigma_{xx,a}$ is the ratio of the amplitudes of normal and shear stresses, δ_{xy} is the phase shift of the shear stress.

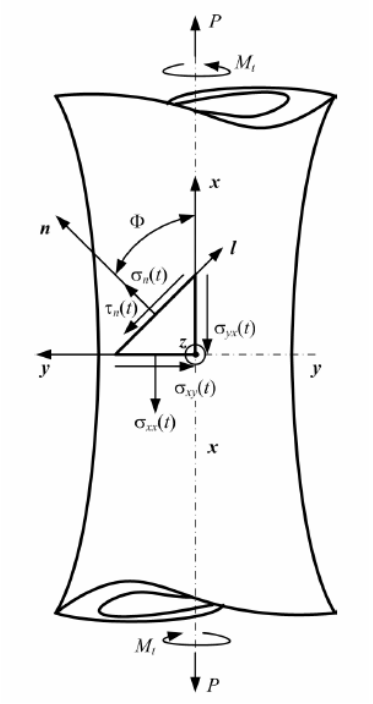

Fig. 1 – Stress state in a point of surface specimen loaded in tension-torsion.

Equations (3) and (4) allow an analysis of the stress states based on two variables, the time moment in the loading cycle (ωt) and the rotation angle (2Φ) respectively, considering two arbitrary parameters: the β ratio and phase shift, δ_{xy}.

Figure 2a shows the Cartesian representations of the normal and shear stresses whose laws of variation are described in equations (1) and (2), for a phase shift of $\delta_{xy} = \pi / 6$. Also, the same loading cycle in coordinates $\sigma_{xx}(t) - \sigma_{xy}(t)$ is shown in Fig. 2b.

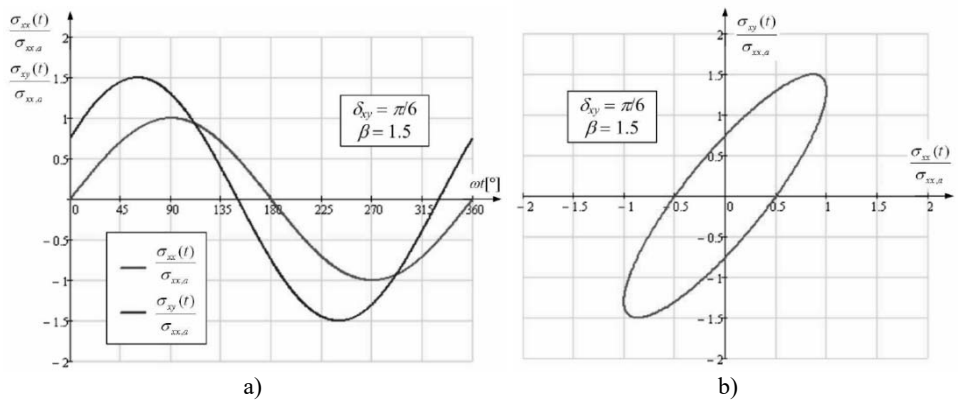

a) b)

Fig. 2 – The tension-torsion loading cycle with a phase shift of $\delta_{xy} = \pi / 6$: a) cartesian coordinates representation; b) $\sigma_{xx}(t) - \sigma_{xy}(t)$ coordinates representation.

The principal stresses are extreme normal stresses acting on the planes with no shear stress. The directions of these stresses are called principal axes. In the same measure, the shear stress registers extreme values in certain planes.

Two cases of determining the maximum principal normal and shear stresses are given in this paper:

Case I. This case involves determining the time in the loading cycle when the normal stress reaches an extreme value in an arbitrary plane rotated by the angle 2Φ. This time moment is given by the following relation:

$$\tan(\omega t) = \frac{1 + \cos(2\Phi) + 2\beta \sin(2\Phi)\cos(2\Phi)}{2\beta \sin(2\Phi)\sin(\delta_{xy})}. \tag{5}$$

The maximum principal stress is:

$$\frac{\sigma_1(2\Phi)}{\sigma_{xx,a}} = \frac{1}{2}\sqrt{A+B},$$

$$A = \left[1+\cos(2\Phi)+2\beta\sin(2\Phi)\cos(\delta_{xy})\right]^2, \tag{6}$$

$$B = \left[2\beta\sin(2\Phi)\sin(\delta_{xy})\right]^2.$$

Also, the time in the loading cycle when the shear stress reaches an extreme value in an arbitrary plane rotated by the angle 2Φ is:

$$\tan(\omega t) = \frac{-\sin(2\Phi)+2\beta\cos(2\Phi)\cos(\delta_{xy})}{2\beta\cos(2\Phi)\sin(\delta_{xy})}, \tag{7}$$

and the maximum shear stress is:

$$\frac{\tau_{max}(2\Phi)}{\sigma_{xx,a}} = \frac{1}{2}\sqrt{\overline{A}+\overline{B}},$$

$$\overline{A} = \left[2\beta\cos(2\Phi)\cos(\delta_{xy})-\sin(2\Phi)\right]^2, \tag{8}$$

$$\overline{B} = \left[2\beta\cos(2\Phi)\sin(\delta_{xy})\right]^2.$$

Case II. This case involves determining the position of the plane for which the normal stress reaches an extreme value at an arbitrary time, (ωt):

$$\tan(2\Phi) = \frac{2\beta\left[\sin(\omega t)\cos(\delta_{xy})+\cos(\omega t)\sin(\delta_{xy})\right]}{\sin(\omega t)}. \tag{9}$$

The maximum principal stress for this case is:

$$\frac{\sigma_1(\omega t)}{\sigma_{xx,a}} = \frac{\sin(\omega t)}{2} + \\ + \frac{1}{2}\left\{\sin^2(\omega t) + 4\beta^2\left[\sin(\omega t)\cos(\delta_{xy}) + \cos(\omega t)\sin(\delta_{xy})\right]^2\right\}^{\frac{1}{2}}. \tag{10}$$

Also, the position of the plane for which the shear stress reaches an extreme value at an arbitrary time, (ωt) is:

$$\tan(2\Phi) = -\frac{\sin(\omega t)}{2\beta\left[\sin(\omega t)\cos(\delta_{xy}) + \cos(\omega t)\sin(\delta_{xy})\right]}, \tag{11}$$

and the maximum shear stress is:

$$\frac{\tau_{max}(\omega t)}{\sigma_{xx,a}} = \\ = \frac{1}{2}\left\{\sin^2(\omega t) + 4\beta^2\left[\sin(\omega t)\cos(\delta_{xy}) + \cos(\omega t)\sin(\delta_{xy})\right]^2\right\}^{\frac{1}{2}}. \tag{12}$$

Based on the above relationships, the variations of the maximum and minimum principal normal stresses, $\sigma_1(t)/\sigma_{xx,a}$ and $\sigma_2(t)/\sigma_{xx,a}$, respectively maximum and minimum principal shear stresses, $\tau_1(t)/\sigma_{xx,a}$ and $\tau_2(t)/\sigma_{xx,a}$, during a loading cycle with $(\omega t)\in[0,2\pi]$, for $\beta = 1$ and different phase shifts, δ_{xy}, were determined and plotted in Figs. 3a–d, respectively Figs. 4a–d.

The analysis of these hodographs of the variation of the principal stresses highlights the difference between a proportional and nonproportional multiaxial loading. During a loading cycle, in Figs. 3a and 4a the variation of the principal stresses is kept on the same principal direction. This variation is characteristic of proportional loadings with phase shift, $\delta_{xy} = 0$. Instead, with the appearance of a phase shift between the applied loadings, the maximum and minimum principal stresses change their mode of variation during a loading cycle. The same happens with the positions of the principal directions that change within the same loading cycle. Such cases are characteristic of nonproportional multiaxial loadings, $\delta_{xy} \neq 0$ (Figs. 3b–d and 4b–d).

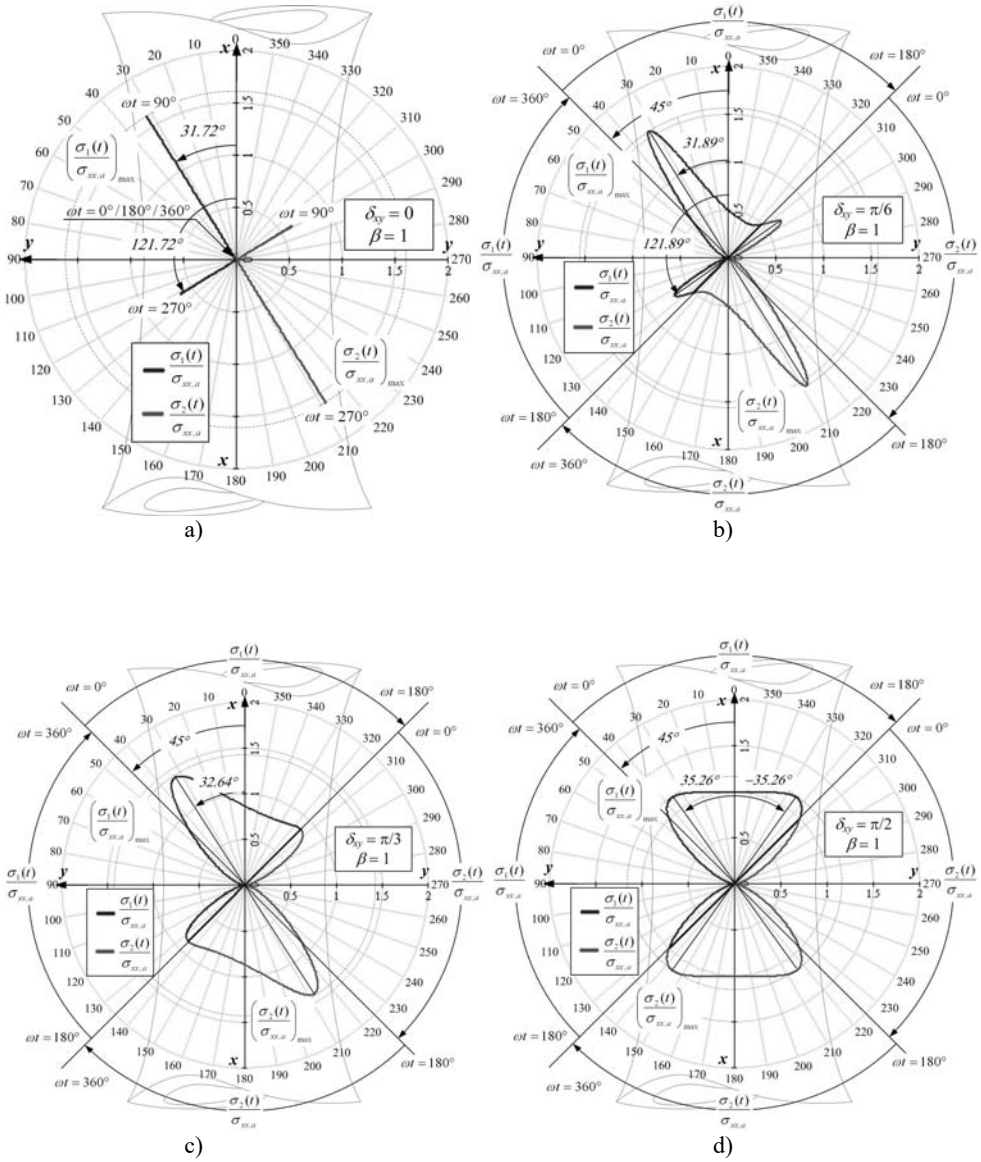

Fig. 3 – Hodograph of the principal normal stresses.

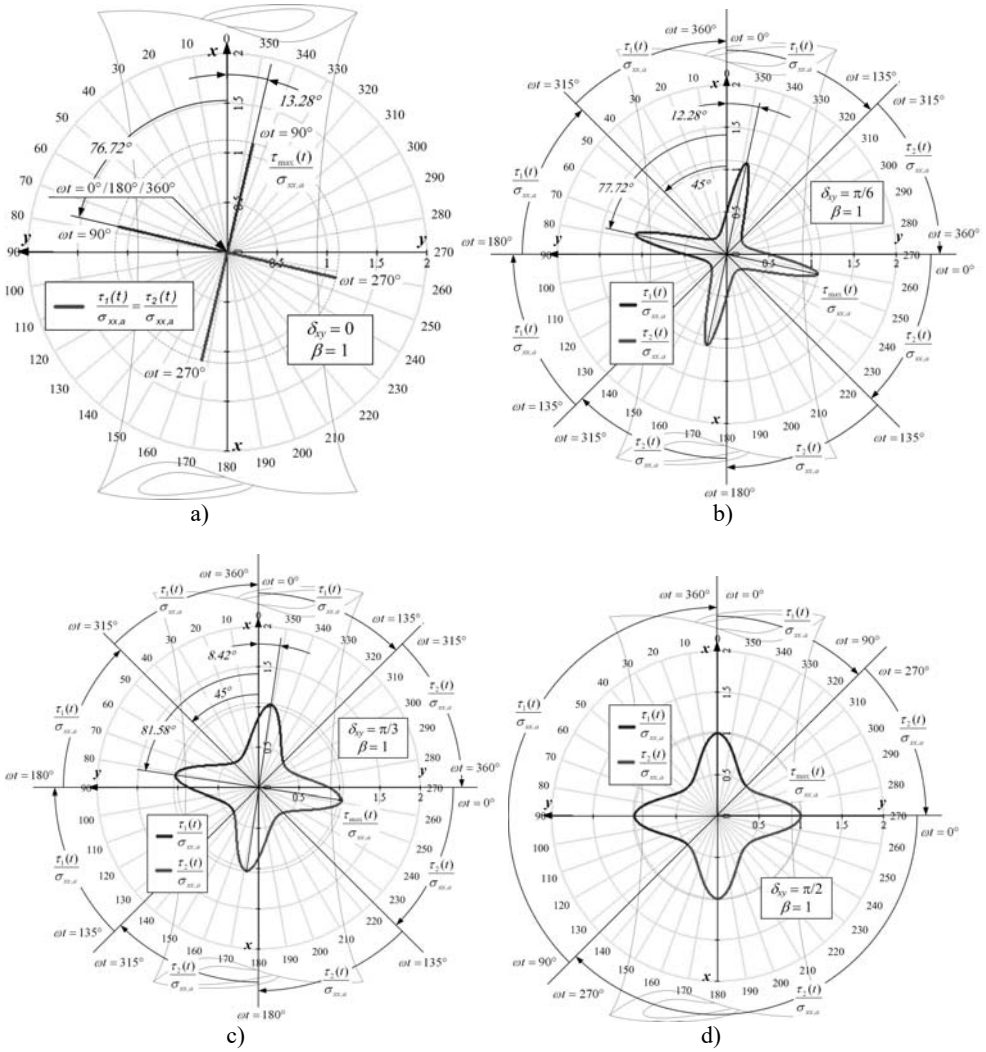

Fig. 4 – Hodograph of the principal shear stresses.

3. FATIGUE DAMAGE PREDICTION IN PROPORTIONAL TENSION-TORSION FATIGUE TESTS

Proportional tension-torsion fatigue tests with stress ratio $R = 0.1$, were conducted on steel tubular specimens with sizes given in Fig. 5. The tested material is a high strength steel whose mechanical properties are given in Table 1. Both axial tension and torsion loadings have followed sinusoidal laws of variations

during a loading cycle. Also, being a proportional multiaxial loading, the phase shift $\delta_{xy} = 0$. The results of the fatigue tests are given in Table 2.

This paper presents a program for estimating the multiaxial fatigue damage produced by a loading cycle. The program is applied for the third test in Table 2, but it is obvious that it can be repeated for all tests.

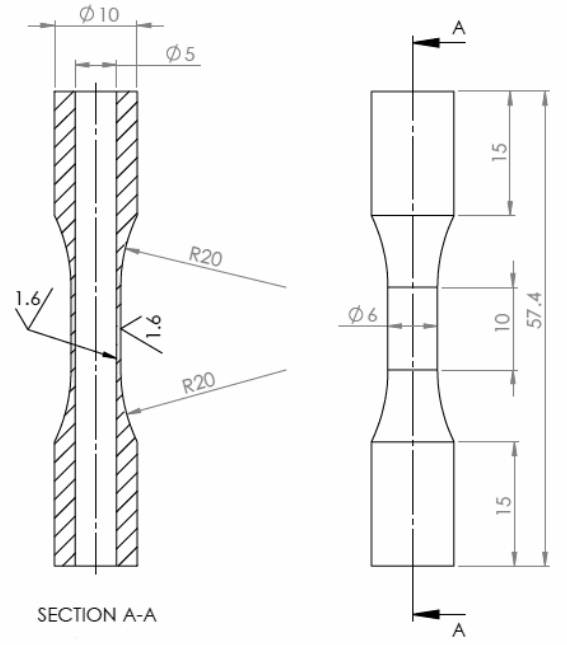

Fig. 5 – Tubular specimen tested for multiaxial fatigue.

Table 1

The mechanical properties of the tested material

Material	**Young's modulus E [MPa]**	**Yield strength σ_y [MPa]**	**Ultimate strength σ_r [MPa]**
High strength steel	205 000	960	1 050

Table 2

The multiaxial fatigue tests

No. test	**Maximum Tensile Force [N]**	**Maximum Torque [Nmm]**	**Cycles to failure**
1	5 353.6	8 500	2 133
2	5 038.7	8 000	5 320
3	4 723.7	7 500	62 674
4	4 408.85	7 000	100 000

First, the maximum and minimum values of the stresses in a cross section will be calculated. Thus:

$$\sigma_{x,max} = \frac{F_{max}}{A} = \frac{4723.7}{8.635} = 547\,\text{MPa}, \tag{13}$$

$$\tau_{xy,max} = \frac{M_{t,max}}{W_p} = \frac{7500}{21.95} = 341.7\ \text{MPa}, \tag{14}$$

where A is the cross-section area and W_p is the strength modulus.

The same calculations are made for the minimum values.

$$\sigma_{x,min} = \frac{F_{min}}{A} = \frac{472.37}{8.635} = 54.7\ \text{MPa}, \tag{15}$$

$$\tau_{xy,min} = \frac{M_{t,min}}{W_p} = \frac{750}{21.95} = 34.17\ \text{MPa}. \tag{16}$$

In the second step, the principal stresses and the angle of the principal directions are determined. These will be calculated both for the maximum values of the normal stress, σ_x, and shear stress, τ_{xy}, respectively for the minimum values. Also, knowing that the maximum values of the normal and shear stresses are recorded at the moment of $\pi/2$, respectively the minimum values are recorded at $3\pi/2$, the principal stresses and the angle of the principal directions are determined using the equations (9) and (10), respectively (11) and (12). All these values are given in Table 3.

Table 3

The principal stresses and direction

	Principal Normal Stress, σ_1 [MPa]	Principal Normal Stress, σ_2 [MPa]	Principal Shear Stress, τ_1 [MPa]	Principal Shear Stress, τ_2 [MPa]	Angle of principal direction, 2Φ [°]
Max.	711.17	–164.17	437.67	–437.67	51.32
Min.	71.11	–16.41	43.76	–43.76	51.32

The stress state corresponding to the analyzed load case is represented in the form of Mohr circles corresponding to its maximum and minimum moments, Fig.6.

Thus, it is considered a plane element on the outer surface of the sample which on the horizontal edges is characterized by the stresses σ_x and τ_{xy} (point A for the maximum moment and A' for the minimum moment in Mohr's circle),

and on the vertical edges only the shear stress τ_{xy} acts (point B for the maximum moment, respectively B' for the minimum moment). Since the angle between the edges is $\pi/2$, the angle between A and B in the Mohr circle is π (always the angle of rotation of the element in the Mohr circle is represented as 2Φ).

Now, there can be estimated the fatigue damage given by the analyzed stress state. This requires the adoption of a damage criterion, and one of the criteria often used in multiaxial fatigue damage prediction is the Findley criterion, [13]. This criterion assumes that a fatigue crack initiation and growth is dependent on both alternating shear stress, $\Delta\tau/2$ and normal stress, σ_n, acting on a plane known as "critical plane".

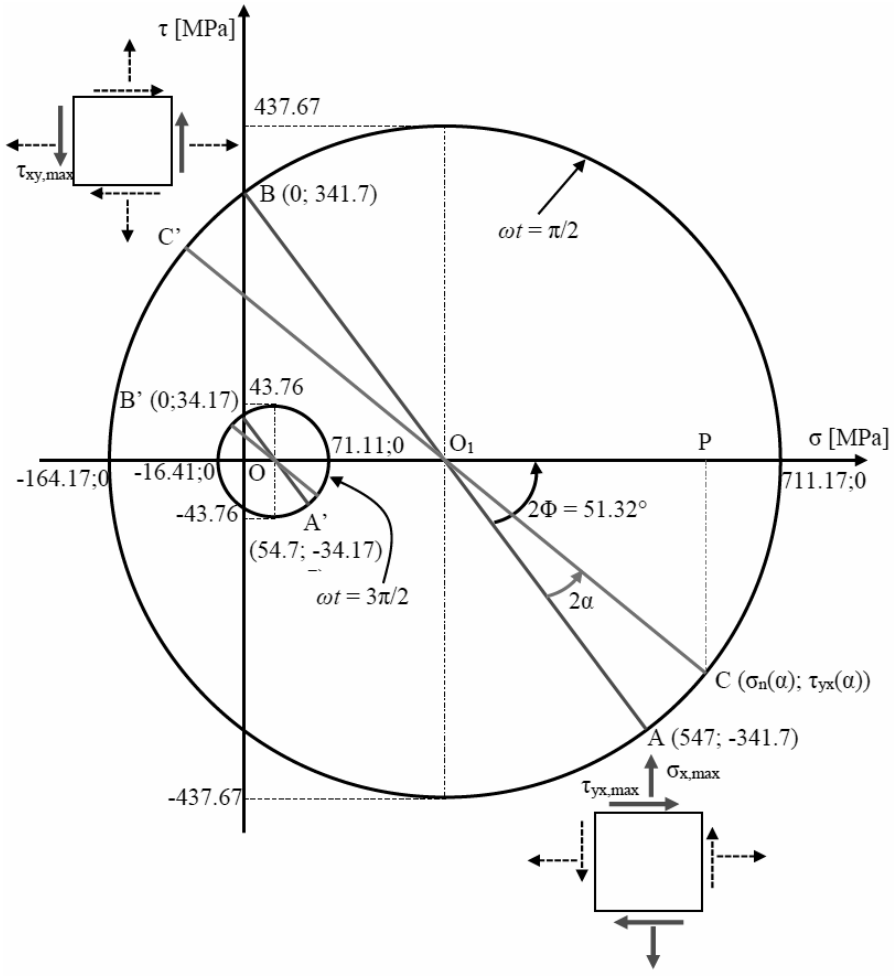

Fig. 6 – The Mohr circles for the maximum and minimum stress states.

The Findley criterion is expressed as:

$$\frac{\Delta\tau}{2} + k \cdot \sigma_n = f_{eff} \tag{17}$$

where k is a Findley constant, that can be estimated based on the following's relationships:

$$k = \frac{1}{\sqrt{\lambda_1 (\lambda_1 - 2)}}, \tag{18}$$

$$\lambda_1 = \frac{2\sigma_r}{\sigma_{-1}}, \tag{19}$$

where σ_{-1} is the fatigue strength at fully reversed cycles which for steels can be estimated as $0.5\sigma_r$.

These stresses must be determined according to the angle of rotation of an element, and for this the Mohr circles in Fig. 6 are used. Thus, a stress state is plotted for a rotated element with an arbitrary angle 2α with respect to the maximum stress state (AB) – Fig. 6. This is represented by the diametrical segment CC'. In the similar way is proceeded on the circle corresponding to the minimum moment.

The normal stress, σ_n is defined as:

$$\sigma_n = OO_1 + O_1P = \\ = \frac{(\sigma_1)_{\max} + (\sigma_2)_{\max}}{2} + \frac{(\sigma_1)_{\max} - (\sigma_2)_{\max}}{2} \cos(2\Phi - 2\alpha). \tag{20}$$

The shear stress corresponding to the maximum moment in the loading cycle is defined from the triangle O_1CP as:

$$CP = (\tau_{xy})_{\max} = \frac{(\sigma_1)_{\max} - (\sigma_2)_{\max}}{2} \sin(2\Phi - 2\alpha). \tag{21}$$

Correspondingly, for the minimum moment the shear stress is:

$$(\tau_{xy})_{\min} = \frac{(\sigma_1)_{\min} - (\sigma_2)_{\min}}{2} \sin(2\Phi - 2\alpha). \tag{22}$$

The shear stress range in a plane rotated by the angle α is given by the following relationship:

$$\Delta\tau = \frac{(\sigma_1)_{max} - (\sigma_2)_{max}}{2}\sin(2\Phi - 2\alpha) - \\ - \frac{(\sigma_1)_{min} - (\sigma_2)_{min}}{2}\sin(2\Phi - 2\alpha). \tag{23}$$

Considering the values given in table 3, for relations (20) and (23), it results:

$$\sigma_n = 273.5 + 437.5 \cdot \cos(51.32° - 2\alpha), \tag{24}$$

$$\Delta\tau = 394 \cdot \sin(51.32° - 2\alpha). \tag{25}$$

Figure 7 shows the variation of the Findley parameter as a function of the rotation angle of the normal to the plane passing through the element whose stress state has been calculated.

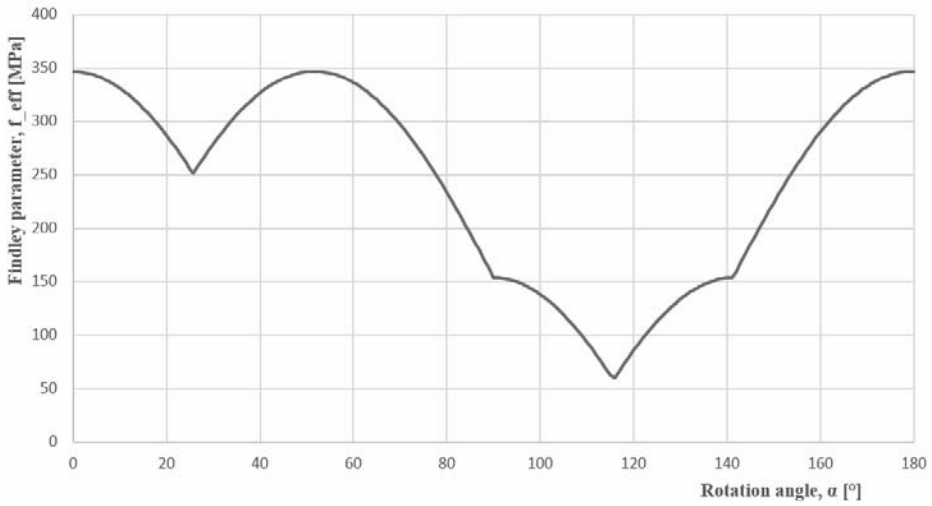

Fig. 7 – The Findley's parameter variation.

For finite fatigue life, the Findley's parameter is often compared with a shear fatigue curve equation as follows:

$$\frac{\Delta\tau}{2} + k \cdot \sigma_n = \tau_f^* \left(N_f\right)^b, \tag{26}$$

$$\tau_f^* = \sqrt{1 + k^2} \cdot \tau_f'. \tag{27}$$

where τ_f' is the shear fatigue strength coefficient, b is the slope of the shear fatigue curve.

In the absence of an experimental torsional fatigue curve, it can be approximated based on the ultimate strength of the material and considering the factors that influence the fatigue strength, [14]. Thus, for the tested material the following coefficients from the shear fatigue curve equation were estimated:

$$\tau'_f = 1\,487.74 \text{ MPa},$$
$$b = -0.139.$$

Also, the fatigue damage produced by a loading cycle is given by the following relation:

$$D_{cycle} = \frac{1}{N_f}. \tag{28}$$

Based on the above relations, figure 8 shows the variation of the fatigue damage produced by a loading cycle depending on the rotation angle of a plane element.

The estimated maximum fatigue damage for the third test corresponds to a fatigue life of 53 778 cycles and occurs for two rotation angles. The rotation angle was measured on Mohr's circle starting from point A, which represents the plane normal on the loading axis of the specimen. The second peak of damage occurs at an angle of 51.66° indicating a second critical plane. The analysis of the failure samples highlights the fact that the fracture was initiated in the transverse plane, Fig. 9. This coincides with the first critical plane indicated by Findley's criterion.

Also, both the estimation of the critical plane and the resulting durability based on Findley's parameter are supported by experimental evidence, which demonstrates the suitability of this criterion for fatigue damage prediction of the analyzed material.

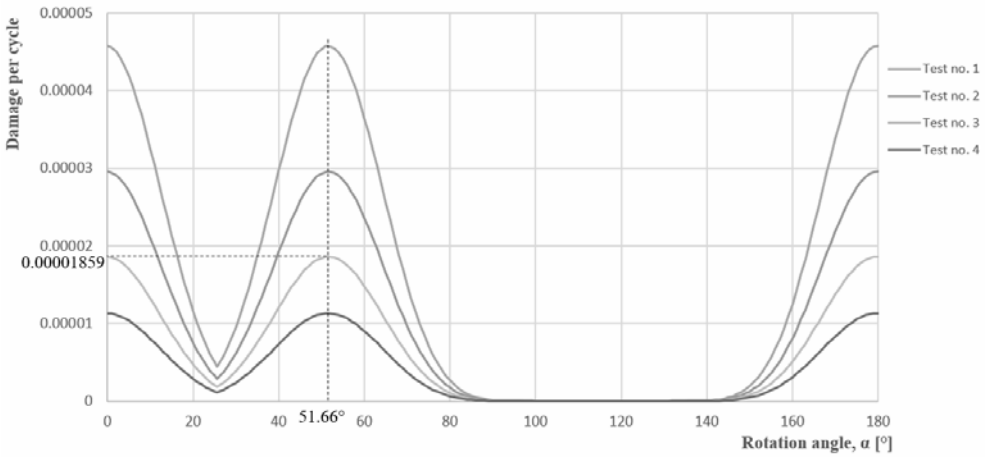

Fig. 8 – Fatigue damage variation depending on the rotation angle of an element.

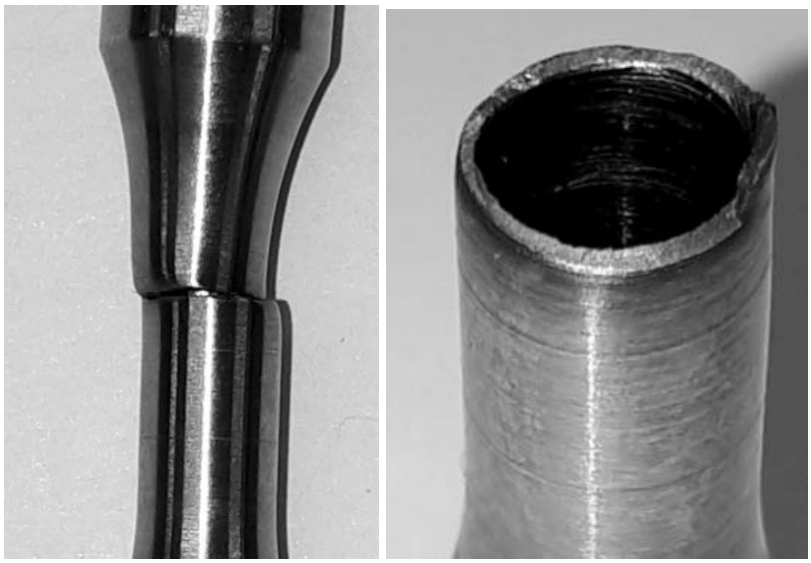

Fig. 9 – Specimen failed by proportional tension-torsion fatigue test.

4. CONCLUSION

A fatigue damage analysis given by a multiaxial proportional tension-torsion cycle is presented in this paper, following a proposed methodology. This methodology is based on the expression of the cyclic stress state through Mohr's circles and the application of a damage criterion, respectively. The fatigue damage variation depending on the rotation angle of the element indicates a sharp peak around the critical plane. This represents a damage concentration on the critical plane emphasizing the initiation of the crack in one of these two critical planes. The fatigue crack initiation in the transverse critical plane, normal on the loading axis, could be influence by the quality of the surface (e.g. roughness).

REFERENCES

1. DUMITRU I., KUN L., SAVA M. *Consideration of the necessity of determining principal stress and direction for analysis of material durability under multiaxial fatigue*, Key Engineering, **601**, pp. 17–20, 2014.
2. KUN L., DUMITRU I., ACHIRILOAIEI D., KUN K., *Influence of phase-shift and amplitude ratio on the principal stress and direction in multiaxial fatigue testing*, Proc. of The 3rd South-East European Welding Congress, Timisoara, Romania, June 3–5, 2015.
3. CERNESCU A., PULLIN R., *New research findings on non-proportional low cycle fatigue*, MATEC Web of Conferences 300, 08003, 2019.
4. SHAMSAEI Nima, McKELVEY Sean, *Multiaxial life predictions in adsence of any fatigue properties*, International Journal of Fatigue, **67**, pp. 62–72, 2014; https://doi.org/10.1016/j.ijfatigue.2014.02.020.

5. SMITH RN, WATSON PP, TOPPER TH, *A stress-strain parameter for fatigue of metals*, J. Mater, **5**, pp. 767–778, 1970.
6. FLAVENOT JF, SKALLI N, *A comparison of multiaxial fatigue criteria incorporating residual stress effects*, Biaxial and Multiaxial Fatigue, EGF 3, edited by M.W. Brown and K.J. Miller, Mechanical Engineering Publications, 1989, pp. 437–457.
7. SOCIE DF, MARQUIS GB, *Multiaxial fatigue*, SAE Inc., 2000.
8. FATEMI A, SOCIE DF, *A critical plane approach to multiaxial fatigue damage including out-of-phase loading*, Fatigue and Fracture Engineering Materials and Structures, **11**, *3*, pp. 149–165, 1988; https://doi.org/10.1111/j.1460-2695.1988.tb01169.x.
9. LEE Y-Li, BARKLEY ME, KANG H-T, *Metal fatigue analysis handbook*, Elsevier Publisher, 2012.
10. CROSSLAND B, *Effect of large hydrostatic pressures on torsional fatigue strength of an alloy steel*, Proceedings International Conference on the Fatigue of Metals, Institution of Mechanical Engineers, London, 1956, pp. 138–149.
11. BANNANTINE JA, SOCIE DF, *Observations of cracking behavior in tension and torsion low cycle fatigue*, Low Cycle Fatigue, ASTM STP 942, H.D. Solomon, G.R. Halford, L.R. Kaisand, B.N. Leis, American Society for Testing and Materials, 1988, pp. 899–921; https://doi.org/10.1520/STP24530S.
12. SOCIE D, *Multiaxial fatigue damage models*, Journal of Engineering Materials and Technology, **109**, *4*, pp. 293–298, 1987; https://doi.org/10.1115/1.3225980.
13. FINDLEY W.N., *A theory for the effect of mean stress on fatigue of metals under combined torsion and axial load or bending*, Journal of Engineering for Industry, 1959, pp. 301–306.
14. LEE Y-Li, PAN J., HATHAWAY R.B., BARKEY M.E., *Fatigue testing and analysis (Theory and practice)*, Elsevier, 2005.